PUBLICATIONS OF THE ASTRONOMICAL SOCIETY OF THE PACIFIC, **122**:745–752, 2010 July

A Photometric Catalog of 77 Newly Recognized Star Clusters in M31

PAUL HODGE

Astronomy Department, University of Washington, Seattle, WA 98195-1850

O. KARL KRIENKE

Seattle Pacific University, Seattle, WA 98119

LUCIANA BIANCHI

Department of Physics and Astronomy, Johns Hopkins University, Baltimore, MD 21218

PHILIP MASSEY

Lowell Observatory, Flagstaff, AZ 86001

AND

KNUT OLSEN

National Optical Astronomy Observatory, Tucson, AZ 85719

Received 2010 May 5; accepted 2010 May 7; published 2010 June 14

ABSTRACT. This paper describes the results of a *Hubble Space Telescope* (*HST*) WFPC2 search for star clusters in active star-formation regions of M31. Nine of the clusters were previously cataloged and 77 are new. Our 23 fields cover key areas of the galaxy's recent star-formation activity. We provide a catalog of positions and integrated magnitudes in four colors, taken with the 336W, 439W, 555W, and 814W filters of the *HST*. A future article will discuss the results of stellar photometry in some of the clusters in six colors, including two additional *uv* colors. The integrated magnitudes and colors of the clusters show a range of characteristics, but the mean color is bluer than for previous surveys, reflecting the concentration of our sample on active star-forming regions. Absolute magnitudes range from $M_{555} = -10.3$ to -3.5. The observed luminosity function shows a nearly Gaussian distribution with a peak value at $M_{555} = -5.4$ and a shoulder of unusually bright clusters. We look in detail at two of these unusually bright examples, cluster 45 (C410) and cluster 10 (BH05). C410 lies at the core of a bright H II region. Its absolute magnitude is $M_{555} = -10.3$. BH05 is a similar object, with an absolute magnitude of $M_{555} = -8.9$. These two clusters are among the most luminous young clusters in M31.

Online material: color figure

1. INTRODUCTION

This paper is part of *HST* Program GO-11079 (PI: L. Bianchi), which was designed to provide six-color data, including three ultraviolet filters, for active star-forming regions in Local Group galaxies (Bianchi et al. 2010). In this article we report on the discovery and photometry of 77 newly recognized star clusters in the fields obtained of M31 (NGC224), together with an additional nine clusters that were previously recognized. We provide cluster positions and measurements of their integrated magnitudes and colors in the *HST* equivalent of U, B, V, and I.

2. OBSERVATIONS

The observations used here were obtained with the *HST's* Wide Field /Planetary Camera 2 (WFPC2). Table 1 lists the 23 positions of the pointings in the disk of M31 used for this article. The targets were chosen to provide data for a representative sample of M31's active star-forming regions and were centered on 20 of van den Bergh's (1964) OB associations. Their positions are plotted in Figure 1. Taking into account a small amount of overlap, the total area searched was 128 arcmin^2, which is approximately 3.0% of the active main disk, as defined by a semimajor axis of 90′ and an axial ratio of 0.2.

At each position 12 exposures were obtained, two for each filter. Filters and exposure times are listed in Table 2. Because the primary purpose of the survey was to achieve uniform signal-to-noise ratios (S/N) across the wavelength coverage (far-UV to I) for the most massive, hottest stars in regions of interest, the exposures for the three longer-wavelength filters

TABLE 1

POSITIONS OF THE *HST* POINTINGS

Name	R.A. (J2000.0)			Decl. (J2000.0)		
	(hr)	(minutes)	(s)	(deg)	(minutes)	(s)
OB10	00	44	10.70	41	33	10.2
OB22	00	41	29.19	40	51	04.3
OB33	00	44	24.26	41	20	49.4
OB39	00	44	35.70	41	25	05.3
OB40	00	44	42.99	41	26	31.3
OB41	00	44	50.10	41	29	06.8
OB42	00	44	57.09	41	31	05.3
OB48N	00	45	16.75	41	39	30.0
OB48S	00	45	10.45	41	37	18.0
OB51	00	45	42.60	41	55	36.3
OB54	00	44	32.78	41	52	16.4
OB59	00	42	59.66	41	37	27.7
OB66N	00	41	28.69	41	13	01.3
OB66S	00	41	24.86	41	12	05.6
OB69	00	40	57.06	41	03	15.4
OB78N	00	40	30.87	40	45	15.6
OB78S	00	40	30.87	40	43	36.6
OB99	00	46	31.35	41	59	22.8
0B102	00	46	33.27	42	11	57.1
OB136	00	39	18.34	40	22	10.4
OB137	00	40	22.96	40	52	40.8
OB139	00	39	43.66	40	20	47.7
OB157	00	47	01.53	42	27	59.6
OB184	00	37	32.77	40	00	44.3

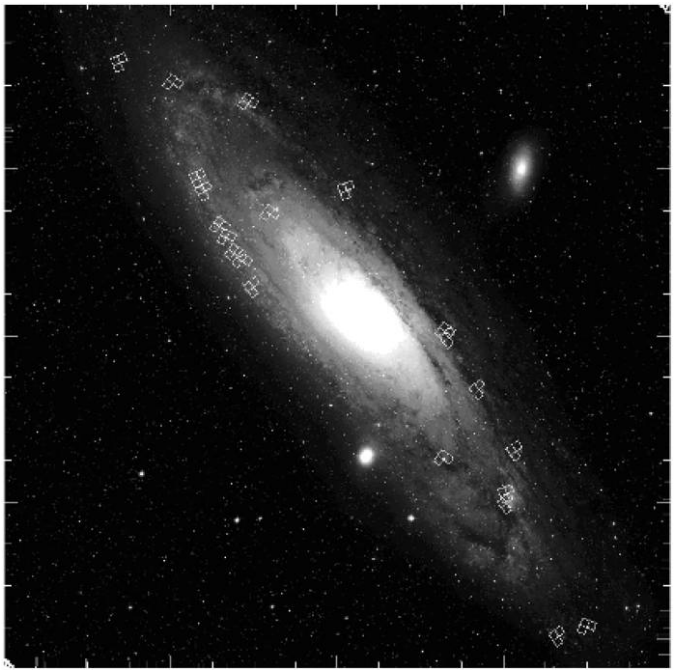

FIG. 1.—Location of the *HST* pointings used for this article, plotted on a blue (*B*) photograph of M31 taken by one of the authors using the Palomar Observatory 1.2 m Schmidt Telescope in 1960. Three outer pointings are beyond the limits of this image, two in the north and one in the south (see Table 1).

TABLE 2

FILTERS AND EXPOSURE TIMES USED FOR THIS CATALOG

Filter	Exposure Time (s)
F336W	2×300
F439W	230+260
F555W	2×50
F814W	2×60

NOTE.—In a few cases, exposures failed and were then repeated.

were short. Consequently, the limiting stellar magnitude at these wavelengths is bright, averaging ~23.7 with the 555W filter.

3. CLUSTER IDENTIFICATION

The images in all colors were examined independently by two of us to identify conspicuous clusters. The selected clusters were limited to objects that showed a significant overdensity of

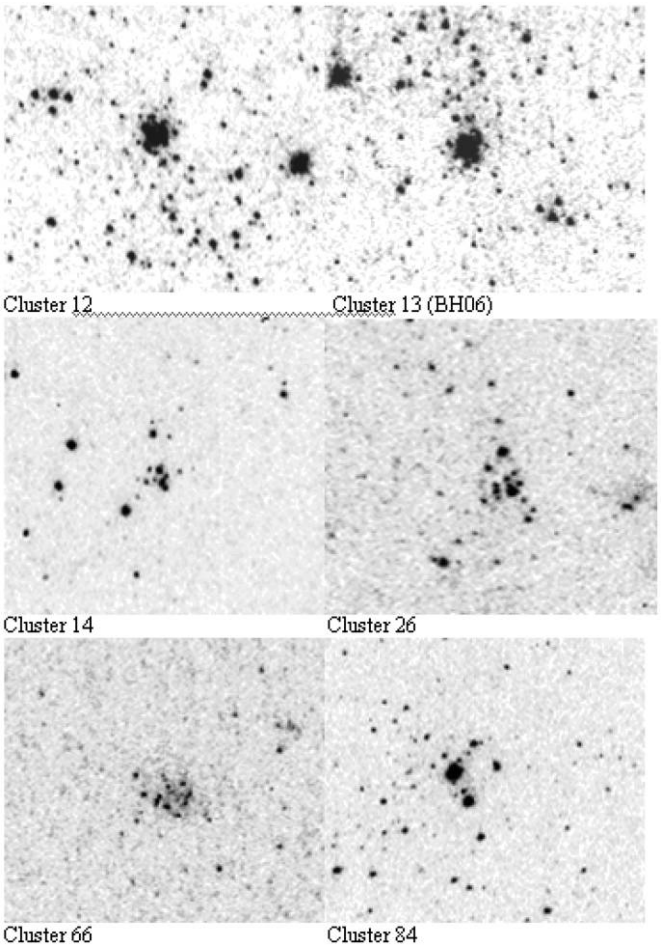

FIG. 2.—Six examples of clusters in the sample. The images are from the F555 exposures and the width of all images is ~14″.

TABLE 3
INTEGRATED MAGNITUDES OF THE CLUSTERS

No.	336	336 error	439	439 error	555	555 error	814	814 error	R.A.	Diam. Decl.	Diam. Pixels	Notes
1	18.22	0.223	19.47	0.21	19.5	0.09	19.53	0.13	9.39204	40.0092	25	
2	16.41	0.125	17.52	0.1	17.23	0.05	16.98	0.1	9.93651	40.3493	49	
3			20.53	0.31	20.15	0.12	19.08	0.14	10.109	40.7588	18	
4	18.85	0.276	18.99	0.16	18.84	0.07	18.31	0.1	10.1136	40.7566	18	*
5	16.86	0.293	18.2	0.46	18.36	0.06	18.34	0.09	10.1142	40.7343	36	
6			19.64	0.19	19.29	0.08	18.41	0.09	10.1163	40.7626	31	
7			21.86	0.33	20.81	0.11	19.53	0.14	10.1234	40.771	21	
8	17.77	0.301	18.64	0.22	18.42	0.08	17.24	0.06	10.1239	40.7331	20	
9	19.23	0.411	20.1	0.29	20.05	0.15	20.31	0.17	10.1262	40.7256	16	
10	15.11	0.058	15.86	0.05	15.82	0.02	15.47	0.04	10.127	40.7581	54	BH05
11	17.03	0.172	17.54	0.11	17.46	0.05	17.22	0.07	10.1272	40.7603	26	
12	16.58	0.152	17.57	0.11	17.61	0.07	17.01	0.05	10.1276	40.7482	31	
13	16.54	0.165	17.38	0.12	17.49	0.06	16.9	0.07	10.1277	40.7484	34	BH06
14	17.65	0.418	18.84	0.28	18.91	0.13	19.05	0.13	10.1289	40.7126	19	
15	18.23	0.442	19.99	0.8	19.89	0.2	20.25	0.35	10.129	40.7262	19	
16			20.32	0.22	19.7	0.08	18.85	0.1	10.1299	40.769	22	
17	18.57	0.861	19.8	0.71	19.83	0.51	19.54	0.8	10.1306	40.7522	17	
18	18.04	0.238	18.94	0.23	19.08	0.08	19.05	0.11	10.1334	40.7449	18	
19	16.52	0.125	17.38	0.09	17.24	0.05	16.68	0.05	10.1337	40.7542	21	
20	17.87	0.218	18.66	0.15	18.45	0.06	17.3	0.05	10.1338	40.7561	29	
21	17.28	0.154	18.6	0.38	18.67	0.2	18.73	0.19	10.1396	40.7211	23	
22	16.67	0.355	17.5	0.12	16.85	0.04	15.95	0.04	10.1421	40.7218	20	
23			20.9	0.42	20.49	0.13	19.8	0.13	10.1456	40.7533	21	
24	0.48		20.28	0.37	19.83	0.11	19.35	0.15	10.228	41.0445	24	*
25			20.96	0.31	20.41	0.11	19.33	0.12	10.2392	41.0673	18	
26	17.7	0.188	18.86	0.16	18.73	0.08	18.52	0.11	10.2435	41.057	31	V212
27			20.2	0.25	20.06	0.1	19.33	0.12	10.3373	41.2001	31	
28			20.21	0.26	19.62	0.1	18.43	0.08	10.3446	41.226	29	
29			20.88	0.3	20.42	0.13	19.04	0.12	10.3499	41.1975	22	
30			21.55	0.36	21.3	0.13	20.33	0.14	10.3572	41.2085	17	
31			20.09	0.23	19.72	0.09	18.86	0.12	10.3594	41.2137	36	
32	18.19	0.23	19.24	0.17	18.8	0.07	16.62	0.04	10.3689	40.8505	26	
33	18.26	0.223	19.09	0.19	18.69	0.07	18.05	0.1	10.3717	41.2212	19	
34	17.03	0.191	17.97	0.11	17.58	0.07	16.93	0.05	10.3734	40.8503	26	*
35	16.84	0.15	17.85	0.13	17.56	0.05	17.18	0.05	10.3736	40.8495	43	
36			20.98	0.33	20.73	0.19	20.07	0.24	10.377	41.2295	21	
37			19.09	0.33	18.66	0.11	17.99	0.12	10.7383	41.623	48	
38			20.32	0.36	19.45	0.11	18.17	0.07	10.7441	41.6021	25	
39	19.84	0.632	20.24	0.38	19.55	0.12	18	0.1	10.7442	41.6149	32	
40	18.31	0.331	18.91	0.21	18.33	0.06	17.43	0.09	10.7581	41.6299	33	
41	20.11	0.468	20.12	0.24	19.23	0.08	18.1	0.08	10.771	41.6218	21	
42			20.88	0.26	20.39	0.09	19.64	0.11	11.056	41.5667	21	
43			21.17	0.28	20.8	0.09	19.99	0.11	11.0588	41.5554	27	
44			20.04	0.25	19.85	0.08	19.63	0.13	11.0895	41.3635	37	
45	15	0.064	16	0.05	15.7	0.02	15.21	0.03	11.1047	41.347	42	C410
46	17	0.208	17.83	0.15	17.44	0.06	16.84	0.07	11.1047	41.3458	32	
47	19.31	0.395	19.87	0.29	19.35	0.11	17.57	0.07	11.1125	41.8676	27	
48	18.83	0.308	20	0.24	19.55	0.09	17.53	0.07	11.1146	41.872	18	
49	19.07	0.337	19.78	0.25	19.54	0.11	19.12	0.15	11.1211	41.8777	21	
50	21.2	2.288	21.44	1.06	20.76	0.34	19.72	0.24	11.1241	41.8654	18	
51	20.41	1.031	21.26	0.68	20.44	0.26	19.28	0.65	11.1255	41.8662	20	
52			21.61	0.85	20.92	0.47	20.15	0.8	11.1289	41.8821	18	
53			20.89	0.31	20	0.09	18.83	0.1	11.1323	41.4198	33	
54	18.02	0.198	18.35	0.15	17.83	0.06	16.89	0.06	11.1324	41.8802	27	
55			19.86	0.34	19.38	0.1	18.68	0.15	11.1353	41.862	42	
56	18.09	0.209	18.44	0.14	17.86	0.05	16.59	0.05	11.1382	41.8865	27	
57	20.5	1.069	20.81	0.5	20.78	0.17	20.07	0.17	11.1395	41.4233	18	

TABLE 3 (*Continued*)

No.	336	336 error	439	439 error	555	555 error	814	814 error	R.A.	Diam. Decl.	Diam. Pixels	Notes
58			21.24	0.59	21.18	0.21	20.51	0.22	11.1401	41.4241	19	
59			19.58	0.46	19.1	0.14	18.32	0.18	11.1406	41.882	29	
60	20.22	0.534	20.89	0.32	20.57	0.13	19.97	0.16	11.1432	41.868	20	
61	17.79	0.185	18.47	0.14	18.3	0.06	17.78	0.07	11.1448	41.8912	32	DAO69
62	19.37	0.45	19.96	0.35	19.38	0.11	17.58	0.07	11.1534	41.8768	19	
63	16.69	0.148	16.68	0.07	16.24	0.02	15.61	0.04	11.1566	41.4205	33	
64	19.91	0.567	20.06	0.26	19.56	0.1	18.72	0.11	11.159	41.8779	20	
65	16.6	0.128	17.51	0.1	17.15	0.04	16.57	0.05	11.1601	41.4198	44	
66			18.91	0.16	18.52	0.07	17.55	0.08	11.1654	41.4077	47	B118D
67			21.19	0.32	20.83	0.13	19.79	0.15	11.1698	41.4127	20	
68			20.33	0.26	20.04	0.09	19.56	0.13	11.1745	41.412	25	
69	18.07	0.218	19.33	0.29	19.34	0.09	19.31	0.14	11.1791	41.439	19	
70			20.78	0.44	20.46	0.15	19.37	0.15	11.2019	41.4798	25	KHM540
71	16.99	0.39	17.74	0.21	17.69	0.09	17.58	0.09	11.2137	41.4906	24	
72			20.83	0.42	19.44	0.1	17.41	0.06	11.2591	41.5219	19	
73			19.36	0.18	19.49	0.08	18.9	0.1	11.2779	41.641	31	KHM566
74	17.15	0.455	18.27	0.21	18.26	0.09	18.23	0.13	11.2931	41.6128	24	
75	16.66	1.11	17.83	0.23	17.4	0.1	16.93	0.13	11.2993	41.6201	57	Nebula
76	17.73	0.308	18.15	0.13	17.58	0.05	16.81	0.05	11.3059	41.6266	28	
77	16.82	0.116	18.12	0.11	18.16	0.05	18.16	0.07	11.323	41.6561	27	
78			20.82	0.37	20.39	0.12	19.94	0.15	11.3316	41.6647	26	
79			20.29	0.24	19.77	0.08	18.9	0.11	11.3378	41.6487	21	
80	20.11	0.706	20.38	0.306	19.99	0.125	19.27	0.147	11.4286	41.9273	44	
81	19.81	0.446	20.04	0.19	19.67	0.08	19.08	0.1	11.4543	41.9316	24	
82	19.32	0.348	19.59	0.21	19.36	0.09	18.76	0.12	11.6233	41.998	21	
83	18.22	0.234	19.21	0.2	19.24	0.09	19.31	0.17	11.6261	42.2105	28	
84	16.67	0.108	18.02	0.1	17.99	0.05	17.89	0.07	11.637	42.2099	17	
85	17.99	0.231	19.08	0.19	18.98	0.09	18.58	0.11	11.638	42.1938	45	
86	18.95	0.364	20.25	0.28	20.01	0.14	19.07	0.15	11.6502	42.0007	22	

stars and an underlying enhanced surface brightness, presumably made up of an unresolved cluster population. The clusters are similar to open clusters in the Milky Way and the more luminous resemble the populous clusters of the Magellanic Clouds. We noted but do not include candidates that did not have a significant number of resolved stars or a tight enough structure, using criteria based on a variety of artificial cluster experiments (described in Krienke & Hodge 2007, hereafter KH07). Sample cluster images are given in Figure 2.

The clusters were first identified as candidates on the F555 images and were then examined on images taken with the other filters. In general, the clusters were most conspicuous on the F555 and F450 images. On some of the F814 images, clusters tended to be almost lost in the sea of red stars of the M31 disk.

4. THE CLUSTER CATALOG

Table 3 is a catalog of the 86 clusters selected. We list their positions and give photometric data for the four filters, as described in § 5. Positions were determined from the F555 images and have accuracies of $\sim 0.2''$, depending on the symmetry and structure of the cluster.

We compared our list with the compilations of Galleti et al. (2004) and Caldwell et al. (2009) and found that five clusters were previously identified there, and two were included in Krienke & Hodge (2008). Table 4 lists these clusters and compares our data with previous photometry (our values were converted to Johnson B and V using the precepts of Holtzman et al. 1995). A preponderance of negative differences is probably the result of our having attempted to determine complete isophotal magnitudes, rather than magnitudes within a certain aperture. An additional known cluster, C410, did not have previous photometry.

5. INTEGRATED PHOTOMETRY

The values for the integrated magnitudes of the clusters listed in Table 3 were obtained using a photometric program written in IDL and described in detail in KH07. The program determines the cluster properties within a contour chosen to include most of the light, but omitting any bright foreground stars. The critical feature of the photometry is determining the background surface brightness. Because many of the clusters have a low surface brightness, the M31 background is often a significant fraction of the measured signal. The flux of the underlying stellar

TABLE 4
COMPARISONS WITH PUBLISHED DATA

Name	B, This Article	B, Published	Difference	V, This Article	V, Published	Difference
BH05				15.75	16.03	−0.28
BH06	17.38	18.54	−1.16	17.49	18.14	−0.65
B118D	18.91	19.58	−0.67	18.52	19.16	−0.64
V212				18.75	19.14	−0.39
DA069				18.3	18.32	−0.02
KH540	20.77	20.55	0.22	20.46	20.03	0.43
KH566	19.22	19.85	−0.63	19.36	19.54	−0.18

population, generally much older than our clusters, is also color dependent; therefore the uncertainty in background subtraction would affect more than just the flux of the cluster. Our program measures a probable background level and determines its uncertainty by sampling several (10 to 24) similarly dimensioned fields on the image. These data are refined by Chauvenet's criterion, rejecting samples with less than 0.02 probability of belonging to the population, which eliminates the possibility of having anomalously high values caused by bright foreground stars. The average of the remaining values of the background is then flux subtracted from the total flux within the cluster contour. The correction to the magnitudes due to the background subtraction was often several tenths of a magnitude. Clearly, the background correction is an important element in this photometry and it was essential that it and its uncertainty be evaluated carefully. The photometric uncertainties provided in Figure 3 and Table 3 include that of the background, which in some cases dominates the uncertainty.

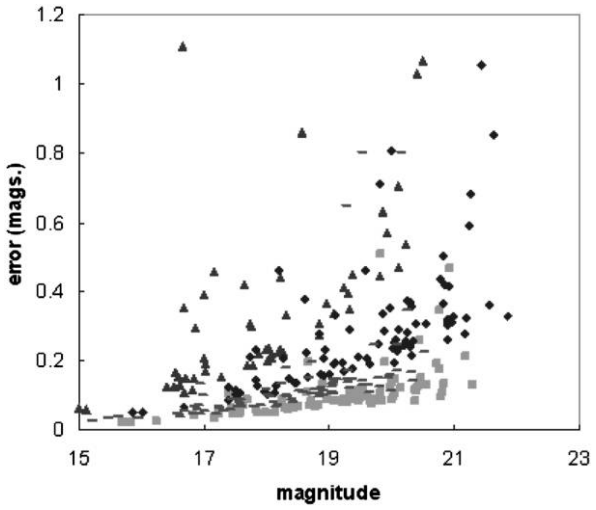

FIG. 3.—Photometric errors for 4 colors. Coding: F336: *triangles*, F439: *diamonds*, F555: *squares*, F814: *dashes*. The large F336 error at magnitude 16.66 is for cluster 75, which is involved in nebulosity. See the electronic edition of the *PASP* for a color version of this figure.

6. COLOR-MAGNITUDE DIAGRAMS

It is useful to plot some of the data in traditional ways, so as to make the overall characteristics of the sample easily comparable to previous studies. Therefore, we present in Figure 4 a (F439, F555) (approximately $B - V$) color-magnitude diagram (CMD) for the integrated measurements for the clusters, uncorrected for reddening. The distribution of points is similar to that of previous surveys of M31 clusters, except that there is a brighter lower luminosity limit, caused by the short exposures of this program, and there are relatively fewer red clusters because of the fact that the pointings are all in active star-forming regions. The mean color of the clusters in this program is $\mathrm{F439} - \mathrm{F555} = 0.334$, while, for comparison, the mean color for a collection of M31 clusters distributed more randomly across the disk and with longer exposures (KH07) was $B - V = 0.501$.

7. THE LUMINOSITY FUNCTION

The luminosity function for the current sample is shown in Figure 5, where it is compared to that for clusters in more

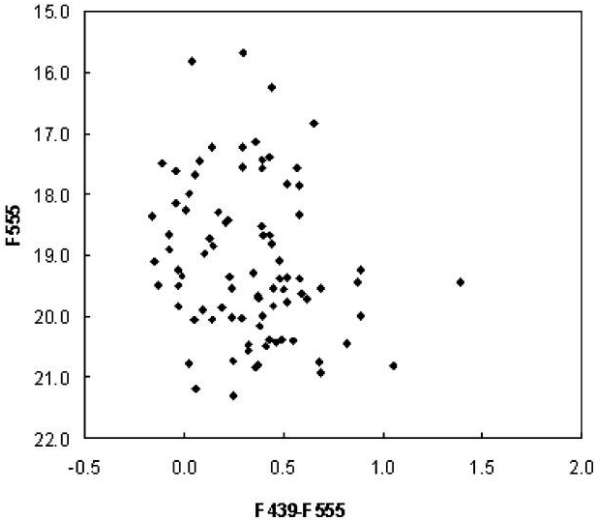

FIG. 4.—F439, F555 CMD (closely comparable to a B, V CMD).

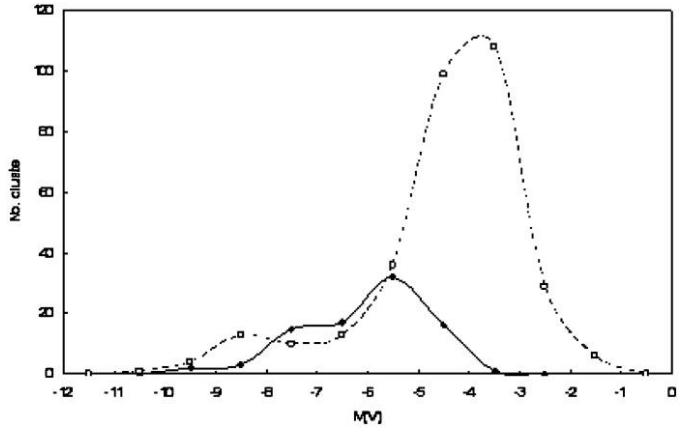

FIG. 5.—Luminosity functions for the present sample of clusters (*solid line*), and for a sample of clusters more randomly distributed across the M31 disk and observed to much fainter limits (Krienke & Hodge 2008, *dashed line*).

general fields in M31, taken from Krienke & Hodge (2008). It is limited to bright clusters by the short exposures of the survey. However, it is useful as a census of M31 star clusters that is restricted to areas of active star formation. The luminosity functions for clusters brighter than $M_V = \sim -5.5$ are very similar (the areas are approximately the same), but the deeper survey detected very many more faint clusters, as expected. Both curves suggest that there is a population of overluminous clusters, compared to the basic quasi-Gaussian shape of the luminosity distribution.

8. REDDENINGS

Mean reddenings were derived by comparison of the integrated colors with Padua (Girardi et al. 2002) single-age cluster models (see Bianchi et al. 2010, for further details). The mean of the different values for the reddenings is 0.28 ± 0.23 (standard deviation). This value agrees well with values found in other samples. For example, Perina et al. (2010), who determined reddenings for 25 young massive M31 clusters using *HST*-based CMDs, found an average of $E(B-V) = 0.276 \pm 0.114$. These values are larger than found for field early-type stars, for which Massey et al. (2007) found an average reddening of $E(B-V) = 0.13 \pm 0.02$.

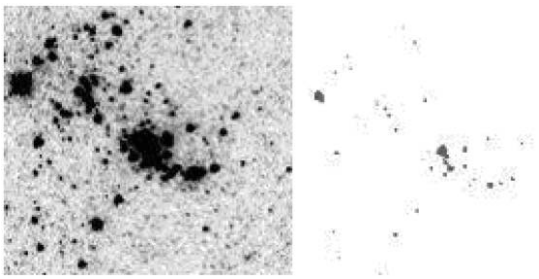

FIG. 6.—Images of cluster 45 (C410) (*center*). The *left* image is from a combined 100 s exposure with the F555W filter. On the *right* is a shallower image at the same scale and from the same exposure, showing the inner stars. The bright central concentration is resolved further into several individual stars. Cluster 46 is above and to the left of cluster 45.

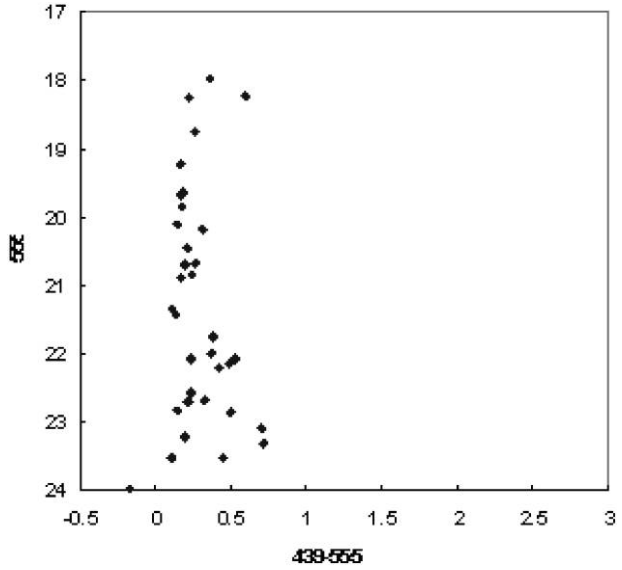

FIG. 7.—Color-magnitude diagram of cluster 45 (C410).

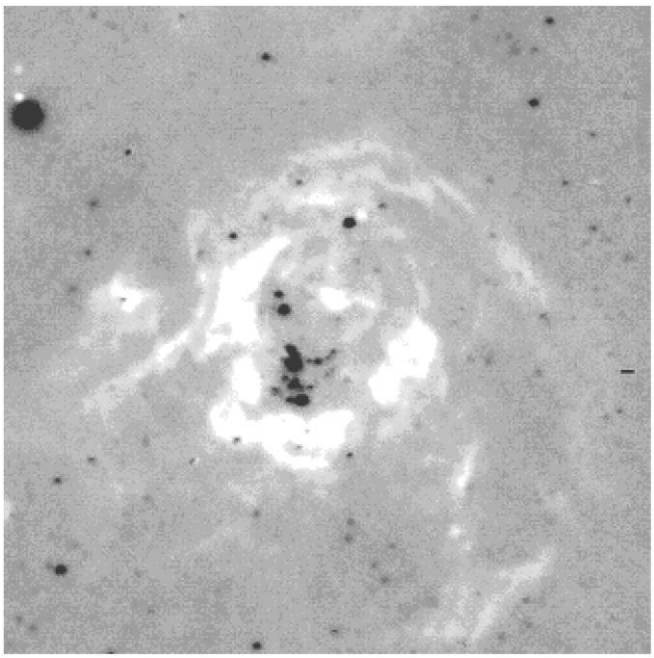

FIG. 8.—H II region Pellet 550 and clusters 45 and 46. In this composite, emission is *white* and stellar continuum is *black*. C410 (cluster 45) is the brightest image at the center of the nearly linear string of stars within and to the left of the center of the H II region. This image was constructed from the images of the NOAO Local Group Galaxies Survey (Massey et al. 2007).

9. THE GIANT CLUSTERS C410 AND BH05

Two of the most luminous clusters in the collection are interesting examples of high-luminosity, massive young clusters, of the sort recognized long ago in the Large Magellanic Cloud and increasingly being discovered in more distant galaxies (Larsen & Richtler 1999). Fusi Pecci et al. (2005) showed that the characteristics of some 15% of the globular clusters in the Revised Bologna Catalog of Globular Clusters in M31 (Galleti et al. 2004) have photometric characteristics suggesting young ages. A recent *HST* CMD survey of these blue globular cluster candidates in M31 showed that most are massive young clusters with ages in the range 25–300 Myr (Perina et al. 2010).

Our cluster 45 was first recognized, apparently, as an unusually bright star cluster during the preparation of the *Atlas of the Andromeda Galaxy* (Hodge 1981), where it was given the designation C410. Images of it and a CMD are given in Figures 6 and 7. In form it consists of a very luminous, compact cluster, surrounded by a more diffuse arrangement of luminous stars. There is a looser, small, but almost equally bright grouping (cluster 46) 4″ to the south, seen in Figure 6, upper left.

C410 has an absolute magnitude of $M_{555} = -10.29$ and a F555–F439 of -0.21 (both corrected for reddening). The CMD (Fig. 7) shows a well-populated luminous main sequence, indicating a very young age.

C410 and cluster 46 are near the center of one of M31's largest H II regions, Pellet 550 (Pellet et al. 1976) (Fig. 8). The large ultraviolet flux from these two objects is circumstantially responsible for the emission region. They are offset from the geometrical center of the larger Hα complex, but close to the locally most luminous emission features (Fig. 9).

The cluster BH05 (Figs. 9 and 10) was discovered by Barmby & Huchra (2001), who identified it as a new globular cluster. Its blue color and its CMD (Fig. 10) indicate that it is instead a massive young cluster. The absolute magnitude M_{555} is -8.89. As shown in the figures, the shape is more elliptical than normal, but this is not unheard of for young massive clusters (e.g., see Perina et al. 2010, for another example in M31).

The CMD of BH-05 (Fig. 10) is similar to that of C410, with a main sequence reaching to an absolute magnitude of $M_{555} = -7.2$. Detailed stellar photometry, including ultraviolet magnitudes, will be presented elsewhere.

The clusters in this survey are primarily young objects, as expected, because of our selection of targets in star-forming areas of M31's disk. We postpone calculation of ages until ultraviolet photometry of the clusters and of their individual stars is available (Bianchi 2009), as the *uv* brightnesses can help to better define the spectral energy distributions of the stars and clusters.

This research was based on observations with the NASA/ESA *Hubble Space Telescope.* Support for *HST* Program GO-11079 was provided by NASA through a grant from the Space Telescope Science Institute, which is operated by the Association of Universities for Research in Astronomy, Inc., under NASA contract NAS5-26555. The CMDs of clusters 10 and 45 were based on HSTphot photometry carried out by Tanya Harrison. We are indebted to the referee, whose prompt and careful report was especially helpful.

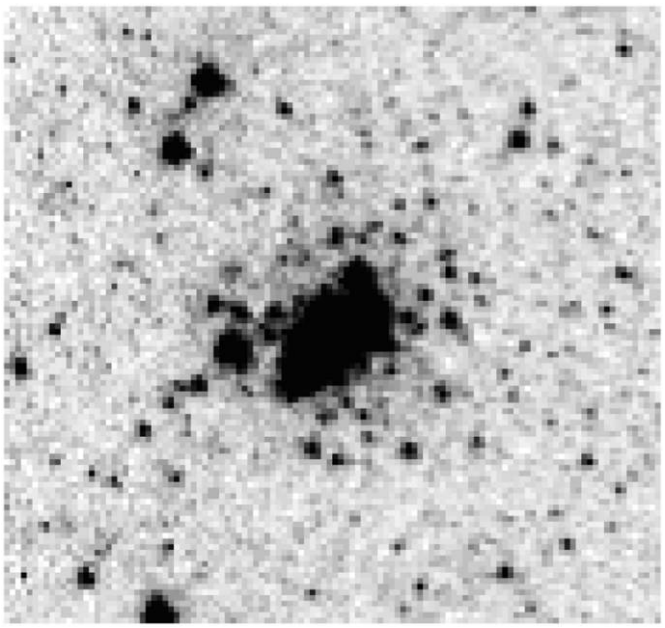

FIG. 9.—F555 image of cluster BH-05 (cluster 10).

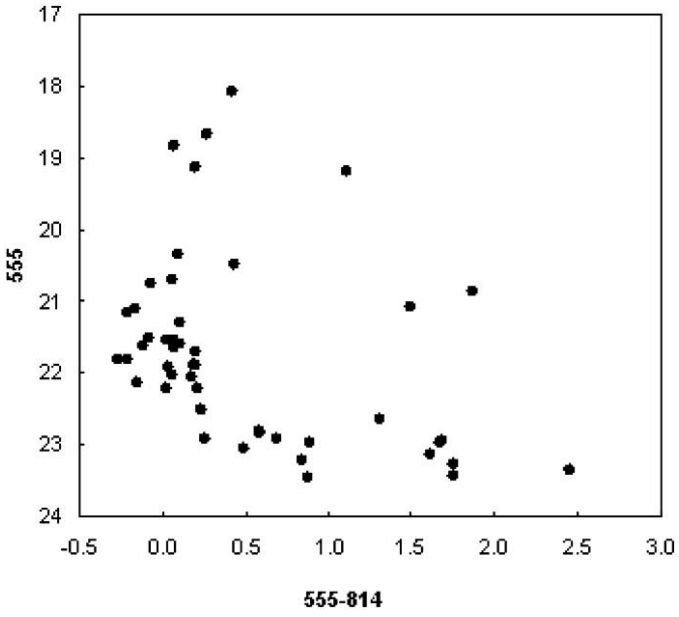

FIG. 10.—Color-magnitude diagram for the cluster BH05 (number 10 in Table 3).

REFERENCES

Barmby, P., & Huchra, J. P. 2001, AJ, 122, 2458
Bianchi, L. 2009, Ap&SS, 320, 11
Bianchi, L., et al. 2010, BAAS, 42, 476
Caldwell, N., Harding, P., Morrison, H., Rose, J., Schiavon, R., & Kriessler, J. 2009, AJ, 137, 94
Fusi Pecci, F., Bellazzini, M., Buzzoni, A., De Simone, E., Federici, L., & Galleti, S. 2005, AJ, 130, 554
Galleti, S., Federici, L., Bellazini, M., Fusi Pecci, F., & Macrina, S. 2004, A&A, 416, 917
Girardi, L., Bertelli, G., Bressan, A., Chiosi, C., Groenewegen, M. A. T., Marigo, P., Salasnich, B., & Weiss, A. 2002, A&A, 391, 195
Hodge, P. W. 1981, An Atlas of the Andromeda Galaxy (Univ. Washington Press: Seattle)
Holtzman, J. A., Burrows, C. J., Casertano, S., Hester, J. J., Trauger, J. T., Watson, A. M., & Worthey, G. 1995, PASP, 107, 1065
Krienke, O. K., & Hodge, P. W. 2007, PASP, 119, 7 (KH07)
———. 2008, PASP, 120, 1
Larsen, S. S., & Richtler, T. 1999, A&A, 345, 59
Massey, P., et al. 2007, AJ, 133, 2393
Pellet, A. 1976, A&A, 50, 421
Perina, S., Bellazzini, M., Barmby, P., Cohen, J. G., Hodge, P. W., Puzia, T. H., & Strader, J. 2010, A&A, 511, 23
van den Bergh, S. 1964, ApJS, 9, 65